The Effect and Mechanism of ROS-Mediated Activation of NLRP3 Inflammasome in Hepatic Alveolar Echinococcosis

caisong chen
Affiliated Hospital of Qinghai UniversityQinghai Province Research Key Laboratory for Echinococcosis
yaogang zhang
Qinghai Province Research Key Laboratory for Echinococcosis
zhixing wang
Affiliated Hospital of Qinghai University
haijiu wang
Affiliated Hospital of Qinghai University
haining fan (fanhaining6@yeah.net)
Qinghai University Medical College

Research

Keywords: ROS, NLRP3 inflammasome, inflammation, hepatic alveolar echinococcosis

Posted Date: July 21st, 2020

DOI: https://doi.org/10.21203/rs.3.rs-44372/v1

Abstract

Background: The NLRP3 inflammasome is a significant component of the innate immune system that plays a vital role in the development of various parasitic diseases. However, its role in hepatic alveolar echinococcosis (HAE) remains unclear. Therefore, we aimed to investigate the NLRP3 inflammasome and its activation mechanism in HAE.

Method: We assessed the expression of NLRP3, Caspase-1, interleukin (IL)-1β, and IL-18 in the inflammatory marginal zone and corresponding normal liver tissues of 60 patients with HAE. We used a rat model of HAE to investigate the role of the NLRP3 inflammasome in the inflammatory marginal zone of HAE. Transwell experiments were conducted to investigate the effect of *Echinococcus multilocularis* in stimulating Kupffer cells and hepatocytes. Further, immunohistochemical staining, western blotting, and ELISA assessed the expression of NLRP3 and Caspase-1, IL-1β, and IL-18, and flow cytometry was used to detect apoptosis and ROS.

Results: The activation of NLRP3 inflammasome was intimately associated with the expression of ROS($P<0.05$). Inhibition of ROS generation decreased the activation of NLRP3-Caspase-1-IL-1β pathway and mitigated damage to hepatocytes ($P <0.01$) as well as inflammation ($P <0.001$) in HAE

Conclusion: *E. multilocularis* can induce hepatocytes damage and inflammatory response by activating the ROS-NLRP3-Caspase-1-IL-1β pathway in Kupffer cells, indicating that ROS may be a potential target for the treatment of HAE.

1 Background

Echinococcosis is a global zoonotic parasitic disease that has two main types, cystic echinococcosis (CE) and alveolar echinococcosis (AE), which are respectively caused by the larvae of *Echinococcus granulosus* and *Echinococcus multilocularis*. AE is also called "parasite cancer" (Xu 2020)[1] and about 80% of AE cases affect the liver, with other organs less frequently infected (Craig 2017)[2]. This disease is mainly prevalent in Asia, Africa, South America, the Middle East, and Australia (Nourbakhsh 2010, Sven 2019)[3, 4]. Humans usually become infected after inadvertently eating the eggs of the worm. The ingested egg hatches in the intestines and is absorbed into the blood through the intestines to reach various organs of the body, where it develops into echinococcosis. Hepatic alveolar echinococcosis (HAE) is a disease that has increased rapidly in recent years. Qinghai Province in China is a region with a high and increasing incidence of echinococcosis (Xiu-Min 2017)[5]. Moreover, epidemiologic evidence demonstrates that the medical and economic burden of HAE will increase drastically in the next decade (Qingling 2014)[6].

The concept of inflammasome was first proposed by Martinon[7] in 2002; its main components include the nucleotide-binding oligomerization domain (NOD)-like receptor family (NOD-like receptors, NLRs) and multiple receptor proteins. Recently, we identified an inflammasome comprising NLRP1, NLRP3, NLRC4

(NLR family CARD domain-containing 4), and AIM2 (absent in melanoma 2).[8]NLRP3 inflammasome has received the most attention. Activated NLRP3 inflammasome can process inactive cysteine aspartate proteolytic enzyme 1 precursor (pro-caspase-1) into active caspase-1; activated caspase-1 can process inactive pro-interleukin (IL)-1β and pro-IL-18 into mature IL-1β and IL-18. Activated NLRP3-caspase-1-IL-18IL-1β pathway exerts biological effects in processes such as stress, inflammatory, and injury repair responses (Hoffman 2001)[9].

The NLRP3 inflammasome is an important participant in inflammatory responses and has been closely associated with inflammation in various liver diseases, including liver cancer (Wei 2014, Saber 2010, Wei 2019)[10–12], viral hepatitis (Ding 2019, McRae 2016)[13, 14], non-alcoholic fatty liver (Sun 2020, Dwivedi 2020)[15, 16], and schistosomiasis (Liu 2019, Chen 2019)[17, 18]. However, the role and clinical significance of the NLRP3 inflammasome in HAE remain unclear. Here, we aimed to explore the activation of the NLRP3 inflammasome in tissues of patients with HAE, rat HAE model, and rat cell models. We investigated the mechanism of NLRP3 inflammasome activation in HAE and the effect of its downstream products on HAE. We hypothesized that *E. multilocularis* might aggravate hepatic damage and inflammation by activating the NLRP3 inflammasome in HAE.

2 Methods

2.1 Parasites and animal experiments

Echinococcus multilocularis was obtained from the Key Laboratory of Echinococcosis in Qinghai Province (Qinghai Province, China)and had been maintained in the laboratory. Eight to ten-week-old male SD rats were used as final hosts. SD rats were purchased from the Nanjing Qinglongshan Laboratory Animal Breeding Centre, China. We inoculated 1200–1500 *E. multilocularis* in the liver of each SD rat[19]to establish HAE rat model. 6-month-old HAE rats were used for experiments. PBN (N-tert-Butyl-α-phenylnitrone; Saint Louis, Missouri, USA) was used as a ROS scavenger in vivo experiments. The efficiency of PBN[20, 21]was tested by treating HAE rats (three rats per group) with three different concentrations—20, 50, and 100 mg/(kg.d)—for 30 days by continuous intraperitoneal injection. Subsequently, PBN 50 mg/(kg.d) group, 50 mg/(kg.d) normal saline (ns) group and control group were established to explore ROS-mediated activation of NLRP3 inflammasome in HAE rats, 10 rats per group. We administered daily intraperitoneal injection to reduce the impact of ROS generation. The feeding and housing were performed in specific-pathogen free (SPF) conditions All experimental procedures were carried out in accordance with the Guide for the Care and Use of Laboratory Animals established by National Health Commission of China.

2.2 Patient tissues

Tissue specimens were collected from 60 patients with HAE who underwent surgery in the Department of Hepatobiliary and Pancreatic Surgery of the Affiliated Hospital of Qinghai University from January 2019 to June 2019. All patients had not received clinical adjuvant therapy, such as radiotherapy, chemotherapy,

and radiofrequency ablation before surgery. All specimens were confirmed to be HAE by pathological examination. The pathological stage and degree of differentiation of the lesions were based on PNM [22]classification criteria. In all patients, the marginal zone of the lesion (less than 0.5 cm away from the lesion) and the tissue adjacent to the lesion (more than 3 cm away from the lesion) were quickly frozen in liquid nitrogen within 15 minutes of surgical resection, and stored in -80 °C. All patients were followed up regularly after surgery. Blood AFP and B-ultrasound were routinely reviewed, and CT was performed if necessary. All patients signed an informed consent and all protocols involving human and animals were approved by Ethics Committee of the Affiliated Hospital of Qinghai University. The experiment started after the approval by Ethics Committee of the Affiliated Hospital of Qinghai University. The Ethical approval number is P-SL-2019054.

2.3 Immunohistochemical staining

Paraffin sections were incubated in 3% H_2O_2 at room temperature for 5–10 min to eliminate the activity of endogenous peroxidase. The sections were rinse with phosphate-buffered saline (PBS) for 5 min. Respective primary antibodies (NLRP3, Abcam, Shanghai, China; Caspase-1, Thermo Scientific, Waltham, MA, USA; IL-18, IL-1β, Boster Biotechnology, Wuhan, China) were added and incubated at 4 ℃ overnight. The sections were rinsed with PBS and further incubated with appropriate secondary antibody (goat anti-rabbit IgG, goat anti-mouse IgG; Beyotime Biotechnology, Shanghai, China) at 20–37℃ for 10–30 min. The optical density and area of all the images were measured by using an Image-Pro Plus 6.0 Image Analysis System (Media Cybernetics, Inc., Bethesda, MD, USA) and the mean density was calculated.

2.4 immunofluorescence staining for cell localization

Paraffin sections were incubated in 3% H_2O_2 to eliminate the activity of endogenous peroxidase. Normal goat serum blocking solution was added to eliminate background staining. The appropriate primary antibodies (CD68, Proteintech, Wuhan, China; NLRP3, Abcam, Shanghai,China;Caspase-1, Thermo Scientific, Waltham, MA, USA) were added and incubated at 4 °C overnight. Sections were washed with PBS and incubated with fluorescent secondary antibody (CY3 Conjugated AffiniPure Goat anti-rabbit IgG, Boster Bio, Wuhan, China) for 2 h. DAPI (Beyotime Biotechnology, Shanghai, China) was added and incubate in the dark for 30 min to stain the nuclei. Cells was observed and images collected under fluorescence microscope (OLYMPUS BX33, JPN).

2.5 Blood biochemical testing

Tail vein blood of the SD rat was collected and WBC, lymphocytes, monocytes levels were measured using a standard hematology analyzer (IDEXX Laboratories Inc., Westbrook, USA)

2.6 Analysis of reactive oxygen species expression and apoptosis by flow cytometry

To detect ROS, Kupffer cells were resuspended with diluted 50 μM DCFH-DA from a reactive oxygen species assay kit (Nanjin Jiancheng Bioengineering Institute, Nanjing, China), and incubated at room temperature for 30 min. For tissue samples, we initially prepared single cell suspension. Liver was

washed with 20 mL PBS, and incubated in 20 mL of type IV collagenase digestion solution (Beyotime Biotechnology, Shanghai, China) at 37 °C. The liver was cut to 2–3 mm^3 with scissors and washed twice with PBS. The single cell suspension were collected for ROS detection.Cells were washed twice with PBS. ROS relative expression was detected through the FITC detection channel (Ex = 500 nm). For apoptosis assay, cells were stained with annexin-V-FITC (MultiSciences,Hangzhou, China) and propidium iodide (PI) according to the manufacturer's instructions.$1–10 \times 10^5$ cells were washed with PBS and resuspended in 500 μl 1 × Binding Buffer. Next, 5 μl Annexin V-FITC and 10 μl PI to each tube. After vortexing gently, the cells were incubated at room temperature in the dark for 5 min. Apoptosis assay was detected through the FITC detection channel and the PI detection channel. Flow cytometry was performed on a FACS calibur (Becton and Dickson, USA). FlowJo (V10.5, Becton and Dickson, USA)was used to analyze the data.

2.7 Co-cultivation experiments

For co-cultivation experiments, normal rat liver cell BRL were purchased from the Institute of Cell Biology of the Chinese Academy of Sciences (Shanghai, China). BRL cells (3×10^5) were plated in the top chamber (6-well; 0.4 μm Pore Polycarbonate Membrane Insert; Corning Life Sciences, Shanghai, China). *E. multilocularis* (1×10^3) and rat liver macrophages (1×10^6) were placed in the lower chamber. Rats BRL hepatocytes, liver macrophages, and *E. multilocularis* were cultured in DMEM (Gibco, Burlington, ON, Canada) medium containing 10% FBS (FBS; Gibco Burlington, ON, Canada). We chose N-Acetyl-L-Cysteine (NAC, Macklin Biochemical, Shanghai, China)as ROS scavenger[23]. After centrifugation at 4,000 rpm for 10 min, the medium supernatant was collected and stored at -80°C, and the co-cultured liver macrophage protein extract was collected. We detected the expression of IL-1β and IL-18 in the supernatant, the expression levels of NLRP3 and Caspase-1 protein in Kupffer cells, and the expression level of ROS in Kupffer cells.

2.8 Western blotting analysis

Protein samples were quantified with the BCA protein assay kit (BIO-RAD, Mississauga, ON, Canada) and subjected to electrophoresis in reducing conditions with poly-acrylamide gels. The proteins were transferred to PVDF membranes. The membranes were blocked for 1 h in TBST (TBS with 0.1% Tween-20) with 5% non-fat milk and incubated with the appropriate antibodies (NLRP3, Abcam, Shanghai, China; Caspase-1, Thermo Scientific, Waltham, MA, USA) overnight at 4°C. After washing, the membranes were blotted with the appropriate HRP conjugated secondary antibody; the blots were developed with ECL reagent from Sangon Biotech (Shanghai, China) in an ImageQuant LAS 4000 image system (GE Healthcare, USA) and analyzed with the Image-Pro Plus 6.0 (Media Cybernetics,, Bethesda, MD, USA). The intensity of bands was normalized to the corresponding values of β-actin.

2.9 ELISA

The ELISA kit (Rat IL-18 ELISA Kit, MultiSciences, Hangzhou, China; Rat IL-1β ELISA Kit, Abcam, Shanghai, China) was used, according to the manufacturer's instructions to determine IL-18 and IL-1β

levels in serum and co-cultured cell supernatant. Each sample was assayed in duplicate and the optical density (OD value) of each well was measured immediately with microplate reader (BIO-RAD iMark, USA).

2.10 Extraction and identification of SD rat Kupffer cell

SD rat liver tissues were washed with 20 mL HBSS (Thermofisher, Shanghai, China) and incubated in 20 mL of type IV collagenase digestion solution (Beyotime Biotechnology, Shanghai, China) at 20–37 °C. Incompletely digested tissues were filtered out and the centrifuged to precipitate liver cells. The supernatant was collected and resuspended in 30% Percoll (Macklin Biochemical, Shanghai, China). The cells in the interface layer were carefully pipetted, diluted with HBSS solution, and the cells collected. For identification, cells were prepared on glass slide cover, fixed with 4% paraformaldehyde for 15 min, and blocked with normal goat serum room temperature for 30 min. Diluted (1:100) primary antibody (CD68 antibody, Proteintech, Wuhan, China) was added and incubated at 4 °C overnight. The slides were washed with PBS and incubated with fluorescent secondary antibody (CY3 Conjugated AffiniPure Goat anti-rabbit IgG, BosterBio, Wuhan, China) at 20–37°C for 1 h. DAPI (Beyotime Biotechnology, Shanghai, China) was added with further incubation in the dark for 5 min to stain the nuclei. Cells were observed and images collected under fluorescence microscope (OLYMPUS BX33,JPN) at magnifications of 200x and 400x.

2.11 Statistical analysis

All statistical analyses were performed by the Graphpad prism 6. Data were analyzed by Student's *t*-test, variance (ANOVA) with Tukey's multiple comparisons test or Wilcoxon test as appropriate. Pearson was used for correlation analysis and Chi-square test was used to analyze the relationship between NLRP3 expression and clinicopathological characteristics of patients with HAE. Quantitative data are presented as the mean ± standard deviation. All P values are two-sided; P value < 0.05 was considered statistically significant;*P< 0.05, **P< 0.01, ***P< 0.001,****P< 0.0001; ns, not significant.

3. Results

3.1 NLRP3 is upregulated in inflammatory marginal tissues and associated with HAE

We found that the H&E stained tissues obtained from patients with HAE had a clear inflammatory marginal zone (Fig. 1A). Immunohistochemical analysis of the expression of NLRP3 in the inflammatory marginal zone tissues and corresponding normal liver tissues of 60 patients with HAE (Fig. 1B), showed that the expression of NLRP3 in the marginal zone was higher than that of the corresponding normal liver tissue (Fig. 1C, P < 0.0001). Using the NLRP3 median expression level (median 0.45) as cut-off, the 60 patients with HAE distributed into a high expression group (n = 30) and a low expression group (n = 30). Clinicopathological analysis showed that the expression of NLRP3 in the marginal zone of HAE was associated with jaundice symptoms (P 0.001) and child-pugh classification (P = 0.012), but was not related to the patient's age, gender, AFP, or primary lesion (all P > 0.05; Table 1). Moreover, to understand the prognostic significance of NLRP3 upregulation in HAE, we analyzed the relationship between NLRP3

expression and survival rate in HAE patients and found that NLRP3 high expression was associated with a poor survival rate (Fig. 1D, P < 0.05).

Table 1

Characteristics	n	NLRP3 low expression	NLRP3 high expression	P value
		n = 30	n = 30	
Age				0.787
≥ 50 years	21	11	10	
< 50 years	39	19	20	
Gender				0.195
Male	33	14	19	
Female	27	16	11	
Serum AFP (ng/mL)				0.796
< 20	32	16	15	
≥ 20	28	14	15	
Jaundice				0.001
Yes	34	8	26	
No	26	22	4	
Primary lesion size				0.0706
≥ 5 cm	51	23	28	
< 5 cm	9	7	2	
Child-pugh grading				0.012
A	42	26	16	
B	18	4	12	

3.2 Expression levels of NLRP3, Caspase-1, and IL-1β are increased in patients with hepatic alveolar echinococcosis

We further carried out immunohistochemical assessments of Caspase-1, IL-1β and IL-18(Fig. 2A) in the marginal zones of the tissues obtained from patients with HAE, compared with normal liver tissues. Expression of Caspase-1 (P< 0.001), IL-1β (P< 0.0001) in the marginal zone were higher than normal liver tissues, but the expression of IL-18 showed no statistical difference (Fig. 2B). We confirmed these finding by western blotting (Fig. 2C, Fig. 2D) that showed higher expression of NLRP3 and Caspase-1 in

the marginal zone compared with normal liver tissues, as shown in Fig. 2E ($P < 0.01$) and Fig. 2F ($P < 0.01$). In addition, we evaluated the relationship between relative expression of NLRP3 and Caspase-1 (Fig. 2G, $P < 0.0001$), NLRP3 and IL-1β relative expression (Fig. 2H, $P < 0.01$), and NLRP3 and IL-18 (Fig. 2I, $P > 0.05$). Taken together, these results indicate that the NLRP3-Caspase-1-IL-1β reaction pathway may be activated in HAE and the activation of the response may play a role in the inflammatory marginal zone. However, IL-18 expression has no correlation with the expression of NLRP3 and Caspase-1.

3.3 ROS is highly expressed in the HAE inflammatory marginal zone and is intimately associated with the activation of NLRP3

We established HAE rat models. The growth of HAE rats is shown in Fig. 3A.We compared the generation of ROS in the marginal zone and normal tissues of HAE rats and observed a relatively higher ROS generation in the marginal zone. About 70.8% of cells in the marginal zone of HAE liver tissues showed high generation of ROS, compared with 31.9% in normal liver tissues (Fig. 3B, Fig. 3C, $P < 0.0001$). The levels of ROS correlated with the relative levels of NLRP3 ,the linear correlation coefficient $r = 0.9489$(Fig. 3D, $P < 0.05$), Thus, we speculated that ROS may play a role in the activation of the NLRP3-Caspase-1-IL-1β reaction pathway in the inflammatory marginal zone of HAE.

3.4 ROS-mediated activation of NLRP3 inflammasome in HAE rats

To further investigate ROS involvement in NLRP3 activation in HAE inflammation, we confirmed that 50 mg/(kg.d) PBN could significantly decrease ROS levels compared to the other concentrations (Fig. 4A). Therefore, 50 mg/(kg.d) PBN was used in subsequent experiments. After 30 days of intervention, we detected generation of ROS in the marginal zone of inflammation in HAE rats of each group (Fig. 4B). We found that white blood cells in the PBN group were significantly decreased compared to NS and control groups (Fig. 4C). Lymphocytes and monocytes were also decreased in the PBN group as shown in Fig. 4D and Fig. 4E. The relative values of inflammatory marginal zone are shown in Fig. 4F. Immunohistochemical analyses of NLRP3, Caspase-1, IL-1β, and IL-18 in the HAE rat marginal zone and normal liver tissues are shown in Fig. 4G. As seen in Fig. 4H, the expression of NLRP3 ($P < 0.001$), Caspase-1 ($P < 0.05$), and IL-1β ($P < 0.05$) in the marginal zone were higher than normal liver tissues, with no statistical difference in the expression of IL-18 ($P > 0.05$). NLRP3 and Caspase-1 protein expression in the marginal zone and normal liver tissues are shown in Fig. 4I with their relative expression (NLRP3 IntDen/β-actin IntDen, Fig. 4J; Caspase-1 IntDen/β-actin IntDen, Fig. 4K). Pearson analysis showed correlation between ROS and NLRP3 expression (Fig. 4L, $P < 0.01$), and between NLRP3 and the inflammation of marginal zone (Fig. 4M, $P < 0.05$), Overall, we observed that NLRP3 expression was closely related to the increase of ROS and inflammation in the marginal zone.

3.5 *Echinococcus multilocularis* activates the NLRP3-Caspase-1-IL-1β pathway through Kupffer cell

We further localized the cells expressing NLRP3 inflammasome and Caspase-1 in the marginal zone of HAE rats as shown in Fig. 5A and Fig. 5B. The results suggest that both NLRP3 inflammasome and Caspase-1 were highly expressed in macrophages (Kupffer cells), but no obvious expression was found in hepatocytes. We asked whether *E. multilocularis* activates the NLRP3-Caspase-1-IL-1β pathway in Kupffer cells by increasing the generation of ROS in Kupffer cells, which increases of IL-1β synthesis and release, leading to hepatocytes damage and promotes acute inflammatory response. In view of this, we isolated rat Kupffer cells, and the identification results are shown in Fig. 5C and 5D. Further, we isolated the *E. multilocularis* in HAE lesions as shown in Fig. 5E. In co-cultures of *E. multilocularis* with Kupffer cells for 24 h, the generation of ROS in Kupffer cells was significantly increased, compared with the control as shown in Fig. 3F($P < 0.01$).

3.6 ROS mediates activation of NLRP3-Caspase-1-IL-18 pathway in Kupffer cells

We chose N-acetylcysteine (NAC) as ROS scavenger to intervene the generation of ROS in a co-culture system, by treating cells with 5, 10, or 20 mM NAC at 24, 48, and 72 h. We observed that 5 mM NAC most efficiently abrogated ROS production in co-cultured cells and thus, the dose was used for further experiments. In transwell co-culture experiments of *E. multilocularis* stimulating Kupffer cells and hepatocytes were set up (Fig. 6B). The generation of ROS in Kupffer cells at 24, 48, and 72 h without or with NAC treatment are shown in Fig. 6C, with obvious suppression of ROS in the NAC-treated co-culture compared to untreated co-cultures (Fig. 6D). Effects on the expression of IL-18 and IL-1β are shown in Fig. 6E and Fig. 6F. Further, we assessed apoptosis of hepatocytes in the co-culture group and the NAC-treated co-culture group at 24 h, 48 h and 72 h as shown in Fig. 6G, with relative levels in Fig. 6H. NLRP3 and Caspase-1 protein expression are shown in Fig. 4I with their relative expression (NLRP3 IntDen/β-actin IntDen, Fig. 4J; Caspase-1 IntDen/β-actin IntDen, Fig. 4K). Altogether, we found that the apoptosis rate and expression of NLRP3 and Caspase-1 were significantly decreased after intervention of ROS generation.

4 Discussion

As a global zoonotic parasitic disease, HAE is rare; however, if not treated, it leads to a high morbidity and mortality, with serious economic burdens. Increasing evidences show that inflammatory processes are crucial for the pathogenesis and progression of serious liver diseases[10, 13, 15]. NLRP3 inflammasome has significant role in the innate immune system involving the inflammatory response[17, 24]. Here, we find that the expression of NLRP3, Caspase-1, and IL-1β in the inflammatory marginal zone of HAE patients are significantly increased. In addition, the results of our in vitro and in vivo experiments show that *Echinococcus multilocularis* activated the ROS-NLRP3-Caspase-1-IL-1β pathway in Kupffer cells, resulting in hepatocyte damage and inflammatory responses.

The inflammatory response is significant in protecting humans and eliminating pathogens. In the presence of harmful external stimuli, inflammation helps remove the stimuli and promote tissue restoration. The activation of inflammatory response is inextricably linked to the activation of the innate immune system. The innate immune response can be activated by a variety of pathogenic organisms through PAMPs (pathogen-associated molecular patterns) or damage-related molecular patterns DAMPs (danger-associated molecular patterns), promoting the release of inflammatory mediators and causing inflammation[25]. NLRP3 inflammasome, as signaling molecules in the innate immune response, has been proven to be involved in tumor development[26, 27] and metastasis [28, 29].In recent years, the role of NLRP3 inflammasome in parasitic diseases has received a wide attention. Santos et al[30]found that the expression of NLRP3 inflammasome was upregulated in malaria. In amoebic disease, the expression of α5β1 integrin in macrophages was related to the activation of NLRP3 inflammasome[31]. Paroli AF et al[32]found that NLRP3 inflammasome and Caspase-1/11 pathway was involved in the host protection against *Trypanosoma cruzi* acute infection. In addition, Gonçalves VM et al[33], found that NLRP3 controlled *T. cruzi* infection through a caspase-1-dependent IL-1R-independent NO production. Further, Lima-Junior DS et al.[34] indicated that inflammasome-derived IL-1β production induced nitric oxide-mediated resistance to *Leishmania*. Ranadhir Deyet al.[35]demonstrated that Leishmaniasis occurred via NLRP3 inflammasome-derived IL-1β. Ritter M et al.[36]found *Schistosoma mansoni* activates the NLRP3 inflammasome and alters adaptive immune responses through Dectin-2. Activation of NLRP3 inflammasomes in mouse resulted in fibrosis of hepatic stellate cells in schistosomiasis.[37] Although the activation of NLRP3 inflammasome seemed different in different parasitic diseases, it is obvious that NLRP3 inflammasome plays some important roles in these diseases. Assessing inflammasomes may help the rapid identification and elimination these pathogenic factors.

NLRP3 inflammasome activation has been related to mitochondrial autophagy and the releasing of ROS[38]. Inhibiting ROS generation or using NADPH (nicotinamide adenine dinucleotide phosphate) oxidase inhibitor can block the activation of NLRP3 inflammasome [39, 40]. As an important participant in oxidative stress, ROS is also closely related to inflammation. Dey et al.[41]found that *T. cruzi* promoted the synthesis and release of ROS, with activation of the NF-κB pathway and decreased expression of inflammatory cytokines in NLRP3 knockout mice, while alleviating acute phase-related symptoms. Shio et al.[42] showed PKC/ROS-mediated NLRP3 inflammasome activation correlated with pathological degree in leishmaniasis. Studies by Gu et al.[43] indicated that specific ROS inhibition and reducing the opening of potassium channels inhibited the expression of NLRP3 inflammasome, suggesting that the release of ROS and the opening of potassium channels are the pivotal factors to activate NLRP3 inflammasome in human prostate epithelial cells. Consistently with previous studies[38, 39], our results indicate that the activation of NLRP3 is intimately associated with the generation of ROS. In addition, ROS-mediated activation of NLRP3 inflammasome plays a vital role in the progression of inflammation in HAE.

IL-1β as an important pro-inflammatory cytokines involved in pathological processes is mainly synthesized by macrophages. It can promote the activation of lymphocytes, macrophages, or NK

cells[44].Apart from these functions, IL-1β is also associated with parasitic infections[34.41]. IL-1β may eliminate these parasite by associating with other components of the immunological system. Our study confirmed that IL-1β was increased in HAE and may be responsible for HAE infection development. In contrast, we did not find an increase in IL-18, possibly because the ROS-NLRP3-Caspase-1-IL-18 pathway was not been activated in HAE.

Notably, mechanistic analysis reveals a novel ROS-NLRP3-Caspase-1-IL-1β signaling pathway regulatory network in HAE inflammatory marginal zone. Further studies are required to address whether there are other inflammasome activated in the HAE inflammatory marginal zone. Moreover, the increase in ROS caused by *E. multilocularis* may be one potential way of NLRP3 activation, and several cross-talk between signaling pathways may also be involved in the regulatory network in this zone. Thus, future efforts should clarify the function and critical mechanisms of immune response in the progression of HAE, which may undoubtedly enhance our understanding of the occurrence and development of the infection and ultimately facilitate the development of diagnosis and therapy for the deadly disease.

5 Conclusions

In present,our work highlights that ROS acts as an activator by promoting inflammatory progression of HAE. Our in vivo experiments showed that inhibiting ROS generation can reduce the activation of NLRP3-Caspase-1-IL-1β pathway. With the expression of IL-1β decreased, inflammation in HAE marginal zone was alleviated. In vitro data revealed significantly decreased apoptosis rates in hepatocyte that corresponded to curbing ROS-NLRP3-Caspase-1-IL-1β pathway in Kupffer cells. Taken together, we concluded that *E. multilocularis* can induce hepatocytes damage and inflammatory response by activating the ROS-NLRP3-Caspase-1-IL-1β pathway in Kupffer cells.

6 List Of Abbreviations

HAE, hepatic alveolar echinococcosis; IL, interleukin; NAC, N-acetylcysteine; NLR, NOD-like receptor; PBN, N-tert-Butyl-α-phenylnitrone; ROS, reactive oxygen species

7 Declarations

Ethical approval and consent to participate

The study complies with the Guide for the Care and Use of Laboratory Animals established by National Health Commission of China. All patients signed informed consent. All protocols involving human and animals were approved by Ethics Committee of the Affiliated Hospital of Qinghai University. The experiment started after the approve by Ethics Committee of the Affiliated Hospital of Qinghai University. Ethical approval number is P-SL-2019054.

Consent for publication

Not applicable.

Availability of data and materials

Data supporting the conclusions of this article are included within the article and its additional files.

Conflict of interest

The authors declare no conflict of interest.

Funding

This project was supported by the National Major Research and Development Project of “Precision Medicine Research”(No.2017YFC0909900), Qinghai Province Science and Technology Department Programme (No.2019-SF-131), and Qinghai province Health and Family Planning Commission Programme (No.2016-wjzd-04).

Authors’ contributions

CCS, WZX,and FHN conceived and designed the experiments.CCS,ZYG, WZX and WHJ collected the samples. CCS,ZYG performed the experiments and data analyses. CCS wrote the first draft of the manuscript, and ZYG and FHN provided comments for revisions. All authors read and approved the final manuscript.

Acknowledgements

Not applicable.

References

1. Xu K, Ahan A. A new dawn in the late stage of alveolar echinococcosis "parasite cancer".Med Hypotheses. 2020 Apr 13;142:109735.DOI: 10.1016/j.mehy.2020.109735.
2. Craig PS, Hegglin D, Lightowlers MW, et al. Echinococcosis: Control and Prevention. Adv Parasitol. 2017;96:55–158. DOI:10.1016/bs.apar.2016.09.002.
3. Nourbakhsh A, Vannemreddy P, Minagar A, et al. Hydatid disease of the central nervous system: A review of literature with an emphasis on Latin American countries. Neurol Res. 2010;32(3):245–51. DOI:10.1179/016164110X12644252260673.
4. Baumann S, Shi R, Liu W, et al. Worldwide Literature on Epidemiology of Human Alveolar Echinococcosis: A Systematic Review of Research Published in the Twenty-First Century Infection. 2019;47(5):703–727. doi: 10.1007/s15010-019-01325-2.
5. Xiu-Min H, Xue-Yong Z, Qi-Gang C, et al. Epidemic status of alveolar echinococcosis in Tibetan children in south Qinghai Province. Zhongguo Xue Xi Chong Bing Fang Zhi Za Zhi. 2017 Feb 13;29(1):53–58.DOI: 10.16250/j.32.1374.2016235.

6. Qingling M, Guanglei W, Jun Q, et al. Prevalence of hydatid cysts in livestock animals in Xinjiang, China. Korean J Parasitol. 2014 Jun;52(3):331–4. DOI:10.3347/kjp.2014.52.3.331.
7. Martinon F, Burns K, Tschopp J. The inflammasome: a molecular platform triggering activation of inflammatory caspases and processing of pro-IL-beta. Mol Cell. 2002;10(2):417–26. DOI:10.1016/s1097-2765(02)00599-3.
8. Harris J, Lang T, Thomas JPW, et al. Autophagy and inflammasomes. Mol Immunol. 2017 Jun;86:10–5. doi:10.1016/j.molimm.2017.02.013.
9. Hoffman HM, Mueller JL, Broide DH,et al. Mutation of a new gene encoding a putative pyrin-like protein causes familial cold autoinflammatory syndrome and Muckle–Wells syndrome. Nat Genet. 2001;29:301–5. DOI:10.1038/ng756.
10. Wei Q, Mu K, Li T, et al. Deregulation of the NLRP3 inflammasome in hepatic parenchymal cells during liver cancer progression. Lab Invest. 2014 Jan;94(1):52–62.DOI: 10.1038/labinvest.2013.126.
11. Saber S, Ghanim AMH, El-Ahwany E, et al. Novel complementary antitumour effects of celastrol and metformin by targeting IκBκB, apoptosis and NLRP3 inflammasome activation in diethylnitrosamine-induced murine hepatocarcinogenesis. Cancer Chemother Pharmacol. 2020 Feb;85(2):331–43. DOI:10.1007/s00280-020-04033-z.
12. 10.3727/096504018X15462920753012
Wei Q, Zhu R, Zhu J, et al. E2-Induced Activation of the NLRP3 Inflammasome Triggers Pyroptosis and Inhibits Autophagy in HCC Cells. Oncol Res. 2019 Jul 12;27(7):827–834.DOI: 10.3727/096504018X15462920753012.
13. Ding X, Lei Q, Li T, et al. Hepatitis B core antigen can regulate NLRP3 inflammasome pathway in HepG2 cells. Med Virol. 2019 Aug;91(8):1528–1536.DOI: 10.1002/jmv.25490.
14. 10.1074/jbc.M115.694059
McRae S, Iqbal J, Sarkar-Dutta M, et al. The Hepatitis C Virus-induced NLRP3 Inflammasome Activates the Sterol Regulatory Element-binding Protein (SREBP) and Regulates Lipid Metabolism. Biol Chem. 2016 Feb 12;291(7):3254-67 DOI: 10.1074/jbc.M115.694059.
15. Sun CC, Zhang CY, Duan JX ,et al. PTUPB ameliorates high-fat diet-induced non-alcoholic fatty liver disease via inhibiting NLRP3 inflammasome activation in mice. Biochem Biophys Res Commun. 2020;19(4):1020–6. DOI:10.1016/j.bbrc.2019.12.131. 523(.
16. Dwivedi DK, Jena GB. NLRP3 inhibitor glibenclamide attenuates high-fat diet and streptozotocin-induced non-alcoholic fatty liver disease in rat: studies on oxidative stress, inflammation, DNA damage and insulin signalling pathway. Naunyn Schmiedebergs Arch Pharmacol. 2020;393(4):705–16. DOI:10.1007/s00210-019-01773-5.
17. Liu X, Zhang YR, Cai C, et al. Taurine Alleviates Schistosoma-Induced Liver Injury by Inhibiting the TXNIP/NLRP3 Inflammasome Signal Pathway and Pyroptosis. Infect Immun. 2019;18(12):87. DOI:10.1128/IAI.00732-19. e00732-19.
18. Chen TTW, Cheng PC, Chang KC, et al. Activation of the NLRP3 and AIM2 inflammasomes in a mouse model of Schistosoma mansoni infection. Helminthol. 2019;15:94:e72.

DOI:10.1017/S0022149X19000622.

19. Liu H, Zhang C. Xiaoxi Fan, et al. Robust Phase-Retrieval-Based X-ray Tomography for Morphological Assessment of Early Hepatic Echinococcosis Infection in Rats. PLoS One. 2017;12(9):e0183396. DOI:10.1371/journal.pone.0183396.
20. Wang B, Xu S, Lu X, et al. Reactive oxygen species-mediated cellular genotoxic stress is involved in 1-nitropyrene-induced trophoblast cycle arrest and fetal growth restriction. Environ Pollut. 2020 May;260:113984. DOI:10.1016/j.envpol.2020.113984.
21. Kim HK1, Park SK, Zhou JL, et al. Reactive oxygen species (ROS) play an important role in a rat model of neuropathic pain. Pain. 2004;111(1–2):116–24. DOI:10.1016/j.pain.2004.06.008.
22. 10.1016/j.parint.2005.11.041
Kern P, Wen H, Sato N, et al. WHO classification of alveolar echinococcosis: principles and application. Parasitol Int, 2006;55:Suppl:S283-S287. DOI: 10.1016/j.parint.2005.11.041.
23. 10.1155/2018/1874985
Xie C, Yi J, Lu J, et al. N-Acetylcysteine Reduces ROS-Mediated Oxidative DNA Damage and PI3K/Akt Pathway Activation Induced by Helicobacter pylori Infection. Oxid Med Cell Longev. 2018;26:2018:1874985. doi: 10.1155/2018/1874985. eCollection 2018.
24. Carretón E, Morchón R, Montoya-Alonso JA. Cardiopulmonary and inflammatory biomarkers in heartworm disease. Parasit Vectors. 2017;10(Suppl 2):534. doi:10.1186/s13071-017-2448-2.
25. Moossavi M, Parsamanesh N, Bahrami A. Role of the NLRP3 inflammasome in cancer. Mol Cancer. 2018;17(1):158. DOI:10.1186/s12943-018-0900-3.
26. Martínez-Cardona C, Lozano-Ruiz B, Bachiller VAI,et al. M2 deficiency reduces the development of hepatocellular carcinoma in mice. Int J Cancer. 2018;1(143(11):2997–3007. DOI:10.1002/ijc.31827.
27. Wei Q, Guo P, Mu K, et al. Estrogen suppresses hepatocellular carcinoma cells through ERβ-mediated upregulation of the NLRP3 inflammasome. Lab Invest. 2015;95(7):804–16. DOI:10.1038/labinvest.2015.63.
28. Dupaul-Chicoine J, Arabzadeh A, Dagenais M,et al. The Nlrp3 Inflammasome Suppresses Colorectal Cancer Metastatic Growth in the Liver by Promoting Natural Killer Cell Tumoricidal Activity. Immunity. 2015;20(4):43. DOI:10.1016/j.immuni.2015.08.013. 751 – 63.
29. Zhang Q, Wang H, Mao C,et al. Fatty acid oxidation contributes to IL-1β secretion in M2 macrophages and promotes macrophage-mediated tumor cell migration. Mol Immunol. 2018;94:27–35. DOI:10.1016/j.molimm.2017.12.011.
30. Santos ML, Reis EC, Bricher PN. Contribution of inflammasome genetics in Plasmodium vivax malaria. Infect Genet Evol. 2016;40:162–6. DOI:10.1016/j.meegid.2016.02.038. 2016.02.038. Epub 2016 Mar 3.
31. Leanne Mortimer F, Moreau S, Cornick. The NLRP3 Inflammasome Is a Pathogen Sensor for Invasive Entamoeba histolytica via Activation of α5β1 Integrin at the Macrophage-Amebae Intercellular Junction PLoS Pathog. 2015;11(5): e1004887. DOI: 10.1371/journal.ppat.1004887.

32. Paroli AF, Gonzalez PV, Diaz-Lujan C, et al. NLRP3 Inflammasome and Caspase-1/11 Pathway Orchestrate Different Outcomes in the Host Protection Against Trypanosoma cruzi Acute Infection. Front Immunol. 2018;39:913. DOI:10.3389/fimmu.2018.00913.
33. Gonçalves VM, Matteucci KC, Buzzo CL, et al. NLRP3 controls Trypanosoma cruzi infection through a caspase-1-dependent IL-1R-independent NO production. PLoS Negl Trop Dis. 2013;7(10):e2469. DOI:10.1371/journal.pntd.0002469.
34. Lima-Junior DS, Costa DL, Carregaro V, et al. Inflammasome-derived IL-1beta production induces nitric oxide-mediated resistance to Leishmania. Nature medicine2013 19: 909–915.DOI: 10.1038/nm.3221.
35. Dey R, Joshi A, Oliveira F. Gut Microbes Egested During Bites of Infected Sand flies Augment Severity of Leishmaniasis Via Inflammasome-Derived IL-1β. Cell Host Microbe. 2018;23(1):134–43. DOI:10.1016/j.chom.2017.12.002. e6.
36. Ritter M, Gross O, Kays S, et al. Schistosoma mansoni triggers Dectin-2, which activates the Nlrp3 inflammasome and alters adaptive immune responses. Proc Natl Acad Sci USA. 2010;107(47):20459–64. DOI:10.1073/pnas.1010337107.
37. Meng N, Xia M, Lu YQ. Activation of NLRP3 inflammasomes in mouse hepatic stellate cells during Schistosoma J. infection. Oncotarget. 2016 Jun 28; 7(26): 39316–39331.DOI: 10.18632/oncotarget.10044. DOI: 10.18632/oncotarget.10044.
38. Afonina IS, Zhong Z, Karin, et al. M Limiting inflammation the negative regulation of NF-κB and the NLRP3 inflammasome. Nature Immunol. 2017;19(8):861–9. DOI:10.1038/ni.3772. 18(.
39. Wree A, McGeough MD, Inzaugarat ME, et al. The NLRP3 inflammasome, a caspase-1 activation platform, plays a key role in the modulation of liver inflammation and fibrosis. Hepatology. 2017. DOI:10.1002/hep.29523.
40. 10.1186/s12974-018-1282-6
Gong Z, Pan J, Shen Q, et al. Mitochondrial dysfunction induces NLRP3 inflammasome activation during cerebral ischemia/reperfusion injury. Neuroinflammation. 2018, 28;15(1):242. DOI: 10.1186/s12974-018-1282-6.
41. 10.1371/journal.pone.0111539
Dey N, Sinha M, Gupta S, Caspase-1/ASC inflammasome-mediated activation of IL-1β-ROS-NF-κB Pathway for Control of Trypanosoma cruzi Replication and Survival Is Dispensable in NLRP3-/- Macrophages. PLoS One. 2014; 9(11): e111539.Published online 2014 Nov 5.DOI: 10.1371/journal.pone.0111539.
42. Shio MT, Eisenbarth SC, Savaria M. Malarial hemozoin activates the NLRP3 inflammasome through Lyn and Syk kinases. PLoS Pathog.2009;5(8):e1000559. Epub 2009. DOI: 10.1371/journal.ppat.1000559.DOI: 10.1371/journal.ppat.1000559.
43. Gu NY, Kim JH, Han IH, et al. Trichomonas vaginalis induces IL-1β production in a human prostate epithelial cell line by activating the NLRP3 inflammasome via reactive oxygen species and potassium ion efflux. Prostate. 2016;76(10):885–96. DOI:10.1002/pros.23178.

44. Yazdi AS, Ghoreschi K. The Interleukin-1 Family. Adv Exp Med Biol. 2016;941:21–9. DOI:10.1007/978-94-024-0921-5_2.

Figures

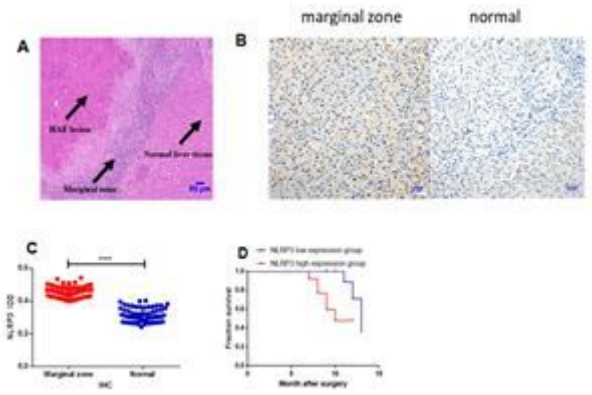

Figure 1

NLRP3 is upregulated in inflammatory marginal tissues and associated with disease progression (A) inflammatory marginal zone of hepatic alveolar echinococcosis. (B) The expression of NLRP3 was immunohistochemically detected in inflammatory marginal zone tissues and corresponding normal liver tissues. (C) Relative expression of NLRP3. (D) prognostic significance of NLRP3 upregulation in HAE (Table1) Correlation analysis of NLRP3 expression and clinical indicators. C, n = 60. D, n = 25.*P < 0.05, **P < 0.01, ***P < 0.001,****P < 0.0001; ns, not significant.

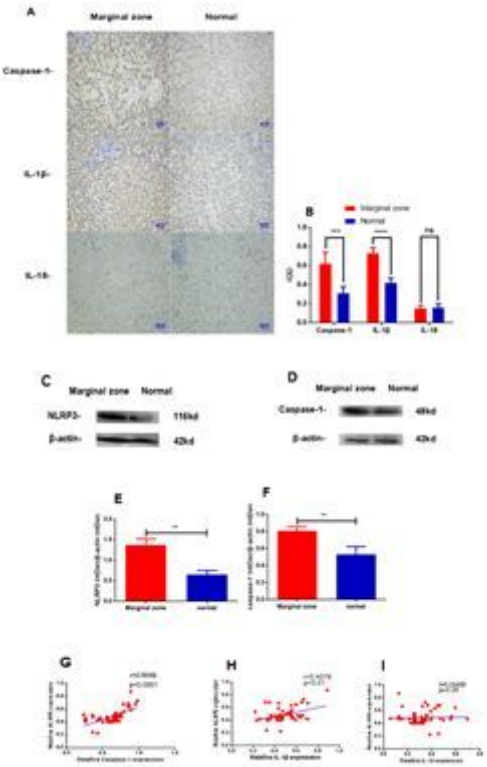

Figure 2

Expression levels of NLRP3, Caspase-1, and IL-1β are increased in hepatic alveolar echinococcosis patients (A) Immunohistochemical detection of Caspase-1, IL-1β and IL-18. (B) Relative expression of Caspase-1, IL-1β and IL-18. (C) NLRP3 protein expression were evaluated by western blotting. (D) Caspase-1 protein expression were evaluated by western blotting.(E)Relative levels of NLRP3 IntDen/β-actin IntDen proteins expression. (F) Relative levels of Caspase-1 IntDen/β-actin IntDen proteins expression. (G) Relationship between NLRP3 and Caspase-1, (H) NLRP3 and IL-1β, (I) NLRP3 and IL-18 relative expression. B–D, G–I, n = 60 per group. The results of western blotting were reproducible in three independent experiments, mean ± SD.*P < 0.05, **P < 0.01, ***P < 0.001,****P < 0.0001; ns, not significant.

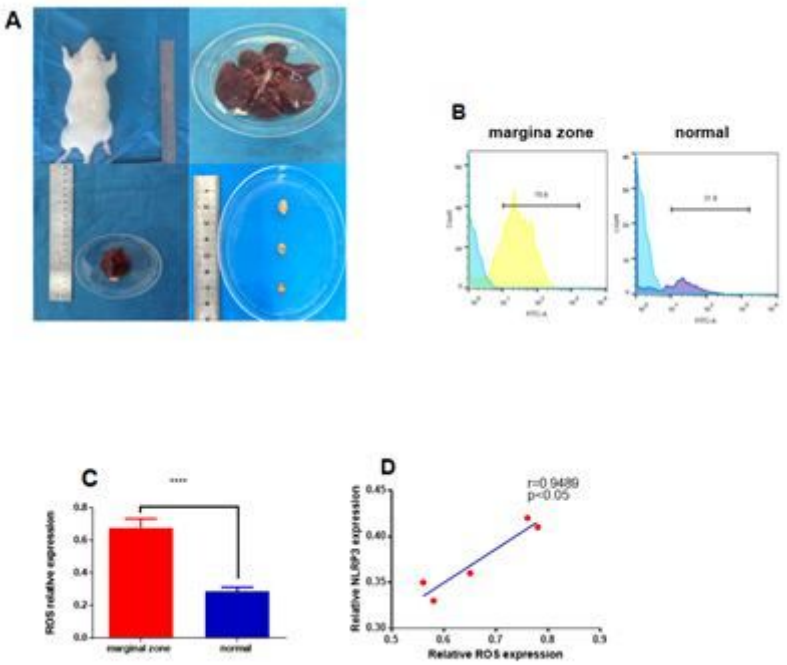

Figure 3

ROS is highly expressed in the HAE inflammatory marginal zone and is intimately associated with the activation of NLRP3 (A)The growth of HAE rats. (B) Generation of ROS in marginal zone and normal tissue. (C) Relative levels of the generation of ROS. (D) Relationship between ROS and NLRP3. C,D, n = 5 rats per group. *P < 0.05, **P < 0.01, ***P < 0.001,****P < 0.0001; ns, not significant.

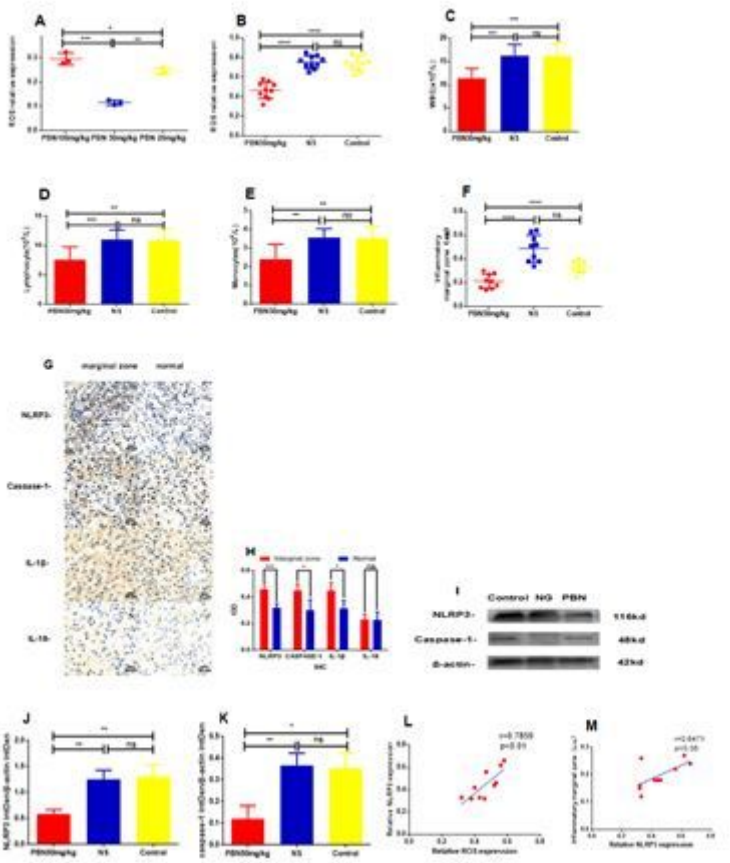

Figure 4

ROS-mediated activation of NLRP3 inflammasome in HAE rats.(A) Result of the generation of ROS in PBN 20 mg/(kg.d) group, PBN 50 mg/(kg.d)group, and PBN 100 mg/(kg.d) group. (B) Result of the generation of ROS in PBN 50 mg/(kg.d) group NS group and control group. (C) WBC in PBN, NS, and control groups. (D) Lymphocytes in PBN, NS, and control groups. (E) Monocytes in PBN, NS, and control groups. (F) Results of inflammation. (G) immunohistochemical detection of NLRP3, Caspase-1, IL-1β, and IL-18. (H) Relative expression of NLRP3, Caspase-1, IL-1β, and IL-18 in the marginal zone comparing with normal liver tissues. (I) Western blotting analyses of PBN, NS, and control group(J) NLRP3 IntDen/β-actin IntDen proteins expression and (K) Caspase-1 IntDen/β-actin IntDen proteins expression. (L) Relationship between ROS and NLRP3 relative expression, (M) NLRP3 relative expression and the inflammation of marginal zone. The results of western blotting were reproducible in three independent experiments, mean ± SD. Scale bar, 50 μm A, n = 3 rats per group; B-F, n = 10 rats per group. L, M, n = 10; *P < 0.05, **P < 0.01, ***P < 0.001,****P < 0.0001; ns, not significant.

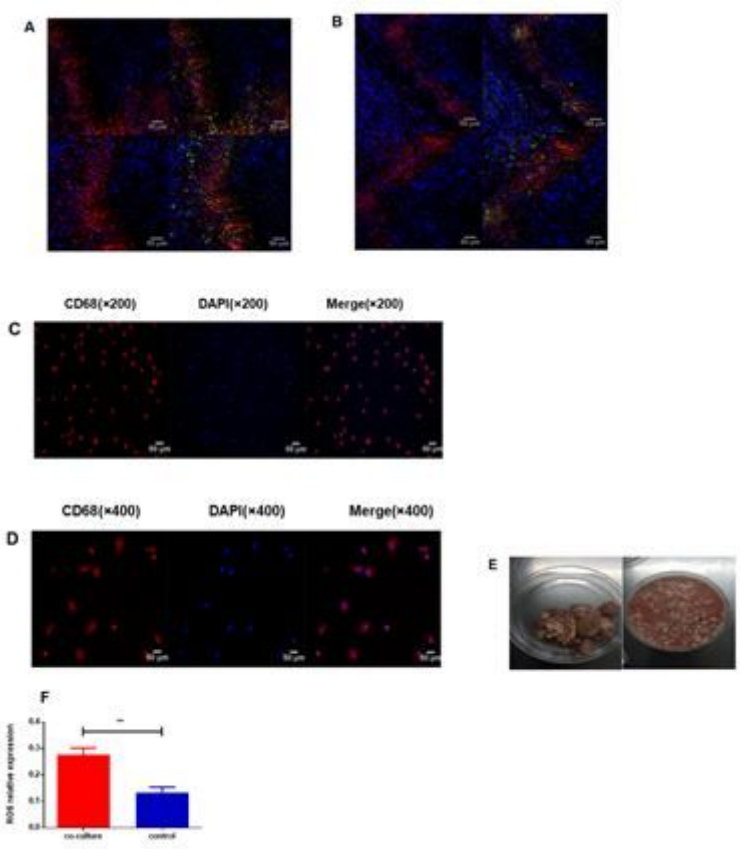

Figure 5

Echinococcus multilocularis activates the NLRP3-Caspase-1-IL-1β pathway in Kupffer cell (A) Cell localization of NLRP3 in the marginal zone (in Fig.5A, red is the NLRP3 inflammasome, blue is the nucleus stained with DAPI, and green is the macrophage marker CD68). (B) Cell localization of Caspase-1 in the marginal zone (in B, red is Caspase-1, blue is the nucleus stained with DAPI, green is the macrophage marker CD68). (C) The identification of Kupffer cells ×200. (D) Identification of Kupffer cells ×400. (in C and D, red is the macrophage marker CD68, blue is the nucleus stained by DAPI, the last image is the fusion picture, E is ×200, F is ×400). (E) Isolation of E. multilocularis (F) Relative expression of co-culture and control groups. Scale bar, 50 □m□F, n = 3, *P < 0.05, **P < 0.01, ***P < 0.001,****P < 0.0001; ns, not significant.

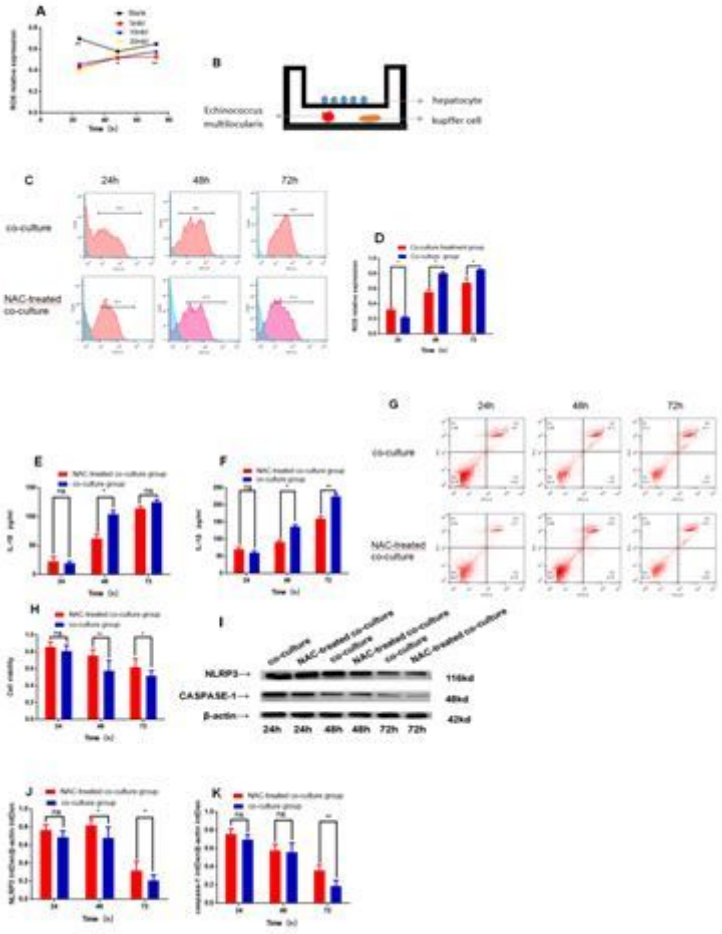

Figure 6

ROS-mediated activation of NLRP3-Caspase-1-IL-18 pathway in Kupffer cells (A) Generation of ROS with the indicated NAC dose at the indicated time points. (B) Representation of transwell model use in the study. (C) Generation of ROS in co-culture group at the indicated time points in the co-culture group and the NAC-treated co-culture group. (D) Relative expression of ROS (E) Expression of IL-18. (F) Expression of IL-1β. (G) Apoptosis of hepatocytes in the co-culture group and the NAC-treated co-culture group at 24, 48, and 72 h .(H) The cell viability of the co-culture group and the co-culture treatment group.(I) Western blotting analyses of indicated proteins. (J) NLRP3 IntDen/β-actin IntDen proteins expression. (K) Caspase-1 IntDen/β-actin IntDen proteins expression. *P < 0.05, **P < 0.01, ***P < 0.001,****P < 0.0001; ns, not significant.